

SUPPLEMENTARY INFORMATION: Overlay databank unlocks data-driven analyses of biomolecules for all

Anne M. Kiirikki¹, Hanne S. Antila^{2,3}, Lara S. Bort^{2,4}, Pavel Buslaev⁵, Fernando Favela-Rosales⁶, Tiago Mendes Ferreira⁷, Patrick F.J. Fuchs^{8,9}, Rebeca Garcia-Fandino¹⁰, Ivan Gushchin¹¹, Batuhan Kav^{12,13}, Norbert Kučerka¹⁴, Patrik Kula¹⁵, Milla Kurki¹⁶, Alexander Kuzmin¹¹, Jesper J. Madsen^{17,18}, Markus S. Miettinen^{2,19,20}, Ricky Nencini¹, Thomas J. Piggot²¹, Ángel Piñeiro²², Fabián Suárez-Lestón^{10,22,23}, and O. H. Samuli Ollila^{1,24,*}

¹University of Helsinki, Institute of Biotechnology, Helsinki, Finland

²Department of Theory and Bio-Systems, Max Planck Institute of Colloids and Interfaces, 14424 Potsdam, Germany

³Department of Biomaterials, Max Planck Institute of Colloids and Interfaces, 14424 Potsdam, Germany

⁴University of Potsdam, Institute of Physics and Astronomy, Potsdam-Golm, 14476, Germany

⁵Nanoscience Center and Department of Chemistry, University of Jyväskylä, P.O. Box 35, Jyväskylä, 40014 , Finland

⁶Departamento de Ciencias Básicas, Tecnológico Nacional de México - ITS Zacatecas Occidente, Sombrerete, Zacatecas, 99102, México

⁷NMR group - Institute for Physics, Martin Luther University Halle-Wittenberg, Halle (Saale), 06120, Germany

⁸Sorbonne Université, Ecole Normale Supérieure, PSL University, CNRS, Laboratoire des Biomolécules (LBM), Paris, 75005, France

⁹Université Paris Cité, UFR Sciences du Vivant, Paris, 75013, France

¹⁰Center for Research in Biological Chemistry and Molecular Materials (CiQUS), Universidade de Santiago de Compostela, Santiago de Compostela, E-15782, Spain

¹¹no affiliation

¹²Institute of Biological Information Processing: Structural Biochemistry (IBI-7), Forschungszentrum Jülich, Jülich 52428, Germany

¹³ariadne.ai GmbH (Germany), Häusserstraße 3 Heidelberg 69115, Germany

¹⁴Department of Physical Chemistry of Drugs and Faculty of Pharmacy, Comenius University Bratislava, 832 32 Bratislava, Slovakia

¹⁵Institute of Organic Chemistry and Biochemistry of the Czech Academy of Sciences, Flemingovo nám. 542/2, Prague, CZ-16610, Czech Republic

¹⁶School of Pharmacy, University of Eastern Finland, 70211 Kuopio, Finland

¹⁷Global and Planetary Health, College of Public Health, University of South Florida, Tampa, Florida, 33612, United States of America

¹⁸Department of Molecular Medicine, Morsani College of Medicine, University of South Florida, Tampa, Florida, 33612, United States of America

¹⁹Department of Chemistry, University of Bergen, 5020 Bergen, Norway

²⁰Computational Biology Unit, Department of Informatics, University of Bergen, 5020 Bergen, Norway

²¹Chemistry, University of Southampton, Highfield, Southampton, SO17 1BJ, United Kingdom

²²Department of Applied Physics, Faculty of Physics, University of Santiago de Compostela, Santiago de Compostela, E-15782, Spain

²³MD.USE Innovations S.L., Edificio Emprendia, 15782 Santiago de Compostela, Spain

²⁴VTT Technical Research Centre of Finland, Espoo, Finland

* samuli.ollila@helsinki.fi

S1 Processing results in the application layer

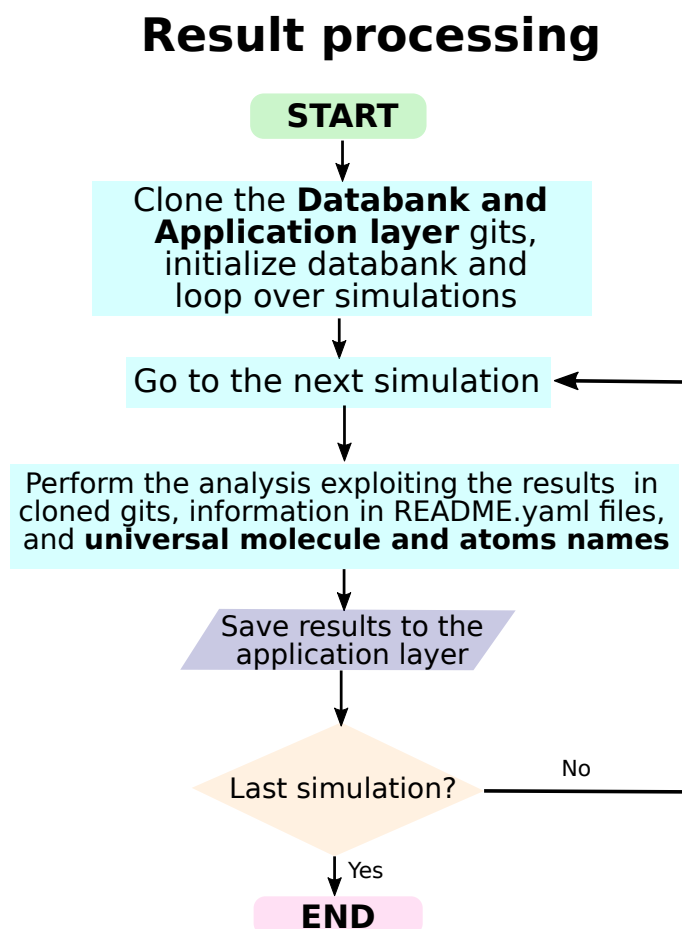


Figure S1. Flowchart for accessing results calculated from the NMRLipids Databank and stored to the *Application layer*.

S2 Correlations of area per lipid and thickness with order parameters and form factors

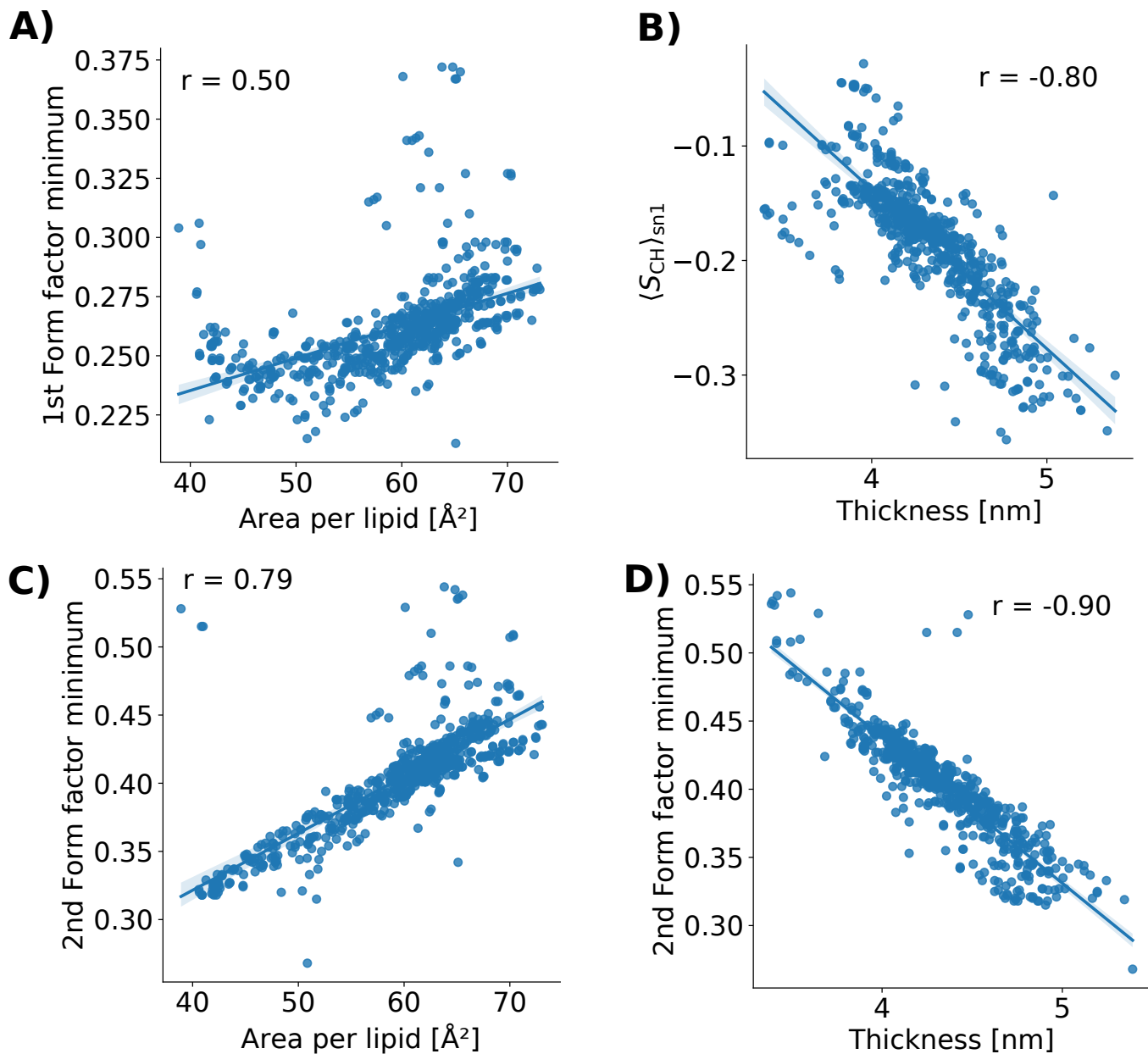


Figure S2. Scatter plots and Pearson correlation coefficients, r , for the membrane area per lipid with X-ray scattering form factor minima (A and B), and for thickness with the average order parameter of the sn-1 acyl chain (B) and with the second minimum from X-ray scattering form factors (D) extracted from the NMRLipids databank. All correlation coefficients have p-value below 0.001.

S3 Dependence of form factor and order parameters on the simulation box size

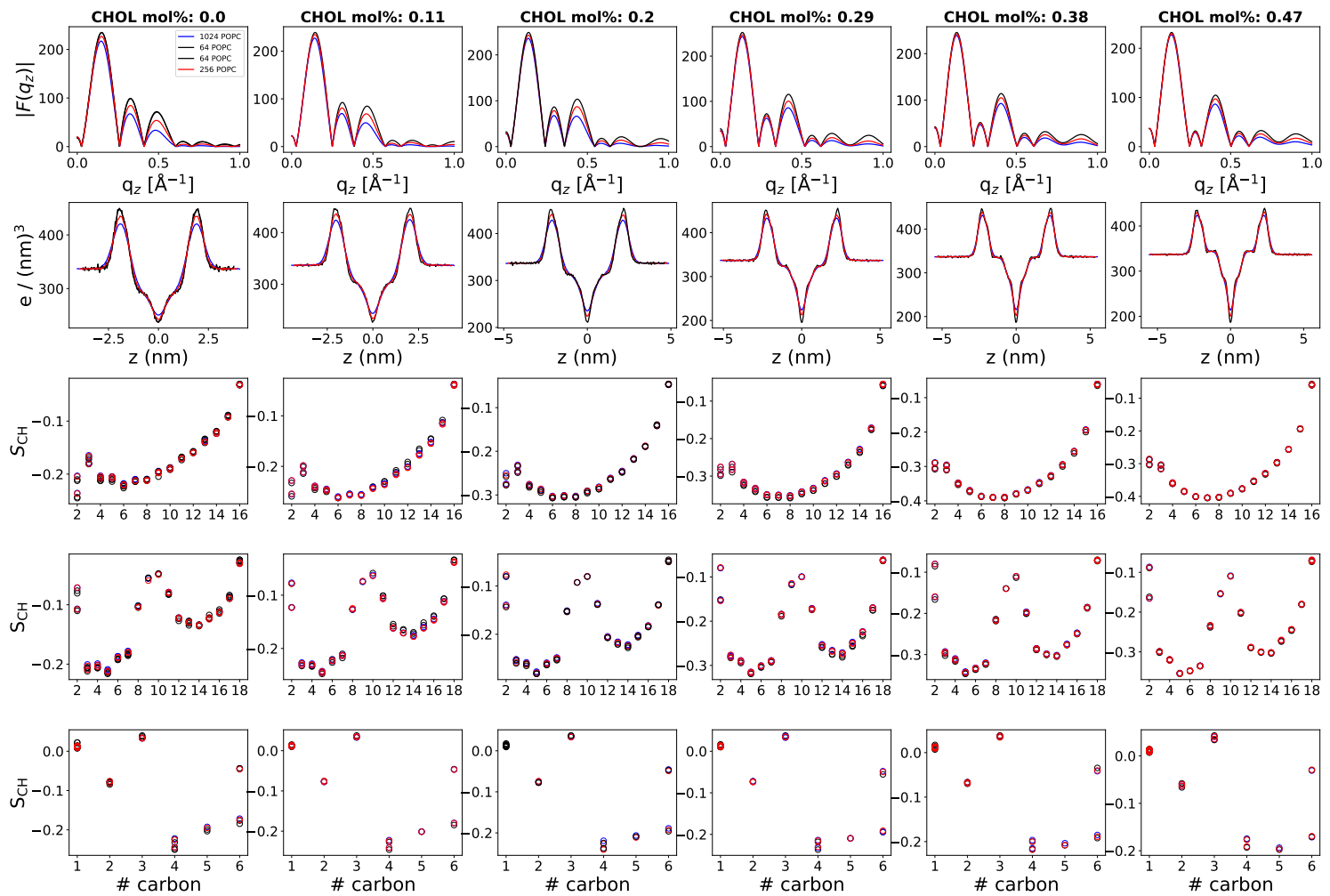


Figure S3. Dependence of the form factor $F(q_z)$, the electron density profiles along membrane normal, and the C–H bond order parameters S_{CH} (from top to bottom) on the simulation box size (with different columns showing different cholesterol concentrations). Simulations with 64, 256, and 1024 POPC lipids are from Ref. 1.

S4 Finding the best models for PC and PE mixtures

| | P^{tails} | P^{hg} | P^{total} | FF_q | τ_{rel} | Force field | Molecules | Temperature | ID |
|----|--------------------|-----------------|--------------------|--------|---------------------|--------------|-------------------------------|-------------|-----|
| 1 | 0.86 | 0.76 | 0.83 | 0.15 | 0.4 | OPLS3e | POPC:SOL (200:8859) | 300.00 | 1 |
| 2 | 0.83 | 0.61 | 0.76 | 0.45 | 7.4 | Slipids | POPC:SOL (512:23943) | 298.00 | 617 |
| 3 | 0.81 | 0.58 | 0.73 | 0.45 | 0.4 | Slipids | POPC:SOL (1024:51200) | 298.15 | 696 |
| 4 | 0.73 | 0.70 | 0.72 | 0.65 | 0.3 | MacRog | POPC:SOL (1024:51200) | 298.15 | 658 |
| 5 | 0.73 | 0.63 | 0.69 | 0.55 | 0.5 | MacRog | POPC:SOL (128:5120) | 300.00 | 457 |
| 6 | 0.76 | 0.54 | 0.69 | 0.55 | 0.4 | Slipids | POPC:SOL (256:12800) | 298.15 | 708 |
| 7 | 0.69 | 0.67 | 0.68 | 0.55 | 0.3 | MacRog | POPC:SOL (256:12800) | 298.15 | 675 |
| 8 | 0.71 | 0.62 | 0.68 | 0.55 | 0.3 | MacRog | POPC:SOL (64:3200) | 298.15 | 674 |
| 9 | 0.69 | 0.54 | 0.64 | 0.76 | 0.4 | Slipids | POPC:SOL (64:3200) | 298.15 | 664 |
| 10 | 0.60 | 0.64 | 0.61 | 0.55 | 7.7 | MacRog | POPC:SOL (288:14400) | 298.00 | 63 |
| 11 | 0.58 | 0.65 | 0.60 | 0.55 | 1.0 | ECC-lipids | POPC:SOL (128:6400) | 300.00 | 573 |
| 12 | 0.66 | 0.47 | 0.60 | 0.15 | 0.2 | Lipid17 | POPC:SOL (64:3200) | 298.15 | 715 |
| 13 | 0.57 | 0.60 | 0.58 | | 0.6 | AMOEBA | DOPC:SOL (72:2880) | 303.00 | 742 |
| 14 | 0.60 | 0.53 | 0.58 | 0.25 | 0.2 | Lipid17 | POPC:SOL (256:12800) | 298.15 | 657 |
| 15 | 0.86 | 0.01 | 0.58 | 0.95 | 0.4 | Berger | POPC:SOL (256:10342) | 300.00 | 115 |
| 16 | 0.58 | 0.54 | 0.57 | 0.25 | 0.2 | Lipid17 | POPC:SOL (1024:51200) | 298.15 | 684 |
| 17 | 0.81 | 0.02 | 0.55 | 1.05 | 1.7 | Berger | POPC:SOL (128:7290) | 298.00 | 497 |
| 18 | 0.49 | 0.65 | 0.54 | 0.76 | 1.1 | ECC-lipids | POPC:SOL (128:6400) | 300.00 | 43 |
| 19 | 0.65 | 0.29 | 0.53 | 0.4 | 1.3 | GROMOS-CKP | POPE:SOL (500:25000) | 310.00 | 400 |
| 20 | 0.78 | 0.01 | 0.52 | 0.1 | 1.3 | Slipids | POPE:SOL (500:25000) | 310.00 | 414 |
| 21 | 0.72 | 0.10 | 0.51 | | 0.7 | Slipids | POPE:SOL (336:13460) | 310.00 | 29 |
| 22 | 0.71 | 0.10 | 0.51 | | 0.8 | Slipids | POPE:SOL (336:13460) | 310.00 | 74 |
| 23 | 0.66 | 0.16 | 0.50 | 0.4 | 0.2 | ECCLipids | POPS:SOL:SOD (72:3600:72) | 298.00 | 443 |
| 24 | 0.38 | 0.67 | 0.48 | 1.26 | 0.7 | CHARMM36 | POPC:SOL (256:9767) | 300.00 | 558 |
| 25 | 0.38 | 0.67 | 0.47 | 1.26 | 0.3 | CHARMM36 | POPC:SOL (1024:51200) | 298.15 | 701 |
| 26 | 0.37 | 0.68 | 0.47 | 1.26 | 0.4 | CHARMM36 | POPC:SOL (200:8880) | 300.00 | 164 |
| 27 | 0.34 | 0.66 | 0.45 | 1.26 | 0.3 | CHARMM36 | POPC:SOL (256:12800) | 298.15 | 710 |
| 28 | 0.40 | 0.54 | 0.44 | 1.3 | 0.2 | CHARMM36 | SOL:POPE (576:144) | 310.00 | 430 |
| 29 | 0.34 | 0.65 | 0.44 | 1.46 | 0.2 | CHARMM36 | POPC:SOL (64:3200) | 298.15 | 678 |
| 30 | 0.55 | 0.21 | 0.44 | 0.8 | 3.2 | GROMOS-CKP | POPS:SOL:SOD (128:4480:128) | 298.00 | 597 |
| 31 | 0.34 | 0.62 | 0.43 | 0.86 | 4.7 | lipid17 | POPC:SOL (128:5120) | 298.15 | 30 |
| 32 | 0.34 | 0.58 | 0.42 | 1.56 | 0.7 | CHARMM36 | POPC:SOL (64:3200) | 298.15 | 546 |
| 33 | 0.55 | 0.15 | 0.41 | 0.8 | 4.9 | GROMOS-CKP | POPS:SOL:SOD (128:4480:128) | 298.00 | 425 |
| 34 | 0.55 | 0.13 | 0.41 | 0.6 | 3.1 | GROMOS-CKP | POPS:SOL:SOD (128:4480:128) | 298.00 | 473 |
| 35 | 0.58 | 0.02 | 0.39 | 0.75 | 2.4 | Berger/Hölte | POPC:CHOL:SOL (120:8:7290) | 298.00 | 305 |
| 36 | 0.41 | 0.32 | 0.38 | 0.3 | 1.0 | CHARMM36-UA | POPE:SOL (336:15254) | 310.00 | 352 |
| 37 | 0.43 | 0.27 | 0.37 | 0.3 | 1.0 | CHARMM36-UA | POPE:SOL (336:15254) | 310.00 | 233 |
| 38 | 0.48 | 0.08 | 0.35 | 0.25 | 6.7 | Orange | POPC:SOL (72:2880) | 298.00 | 38 |
| 39 | 0.39 | 0.20 | 0.33 | 0.7 | 3.8 | GROMOS-CKP | POPS:SOL:SOD (128:4480:128) | 298.00 | 535 |
| 40 | 0.40 | 0.06 | 0.29 | 0.8 | 3.1 | Charmm-Drude | POPE:SOL (144:5040) | 310.00 | 731 |
| 41 | 0.33 | 0.17 | 0.28 | 0.76 | 5.8 | Chiu Gromos | POPC:SOL (128:3552) | 298.00 | 422 |
| 42 | 0.40 | 0.02 | 0.27 | 0.27 | 2.6 | Berger/Hölte | POPC:CHOL:SOL (110:18:8481) | 298.00 | 589 |
| 43 | 0.11 | 0.53 | 0.25 | 1.7 | 1.7 | CHARMM36 | SOL:POPE (25000:500) | 310.00 | 67 |
| 44 | 0.29 | 0.12 | 0.23 | | 5.6 | Slipids | POPG:SOL:SOD (288:10664:288) | 298.00 | 207 |
| 45 | 0.20 | 0.18 | 0.21 | 3.39 | 1.7 | slipids | CHOL:POPC:SOL (256:256:20334) | 298.00 | 82 |
| 46 | 0.25 | 0.07 | 0.19 | 1.36 | 1.0 | GROMOS-CKP | POPC:SOL (500:25000) | 298.00 | 202 |
| 47 | 0.24 | 0.09 | 0.19 | 1.6 | 1.3 | Lipid17 | POPE:SOL (500:25000) | 310.00 | 195 |
| 48 | 0.21 | 0.11 | 0.18 | 0.3 | 2.5 | Slipids | POPS:SOL:SOD (128:4480:128) | 298.00 | 529 |
| 49 | 0.17 | 0.21 | 0.18 | 3.8 | 0.3 | AMOEBA | POPE:SOL (72:2880) | 310.00 | 730 |
| 50 | 0.12 | 0.26 | 0.17 | 0.8 | 3.0 | CHARMM36-UA | POPS:SOL:SOD (128:4480:128) | 298.00 | 263 |

Figure S4. Top 50 simulations in the NMRLipids Databank ranked based on the C–H bond order parameter quality against experiments. The columns 2–4 show qualities for acyl chain order parameters (P^{tails}), headgroup order parameters (P^{hg}), all order parameters (P^{total}), and for X-ray scattering form factors (FF_q). Column 5 shows relative equilibration times for conformations (τ_{rel}). Note that the best possible order parameter quality is one, while the best possible form factor quality is zero. ID values in the last column can be used to identify each simulation in the databank.

Increasing area per lipid

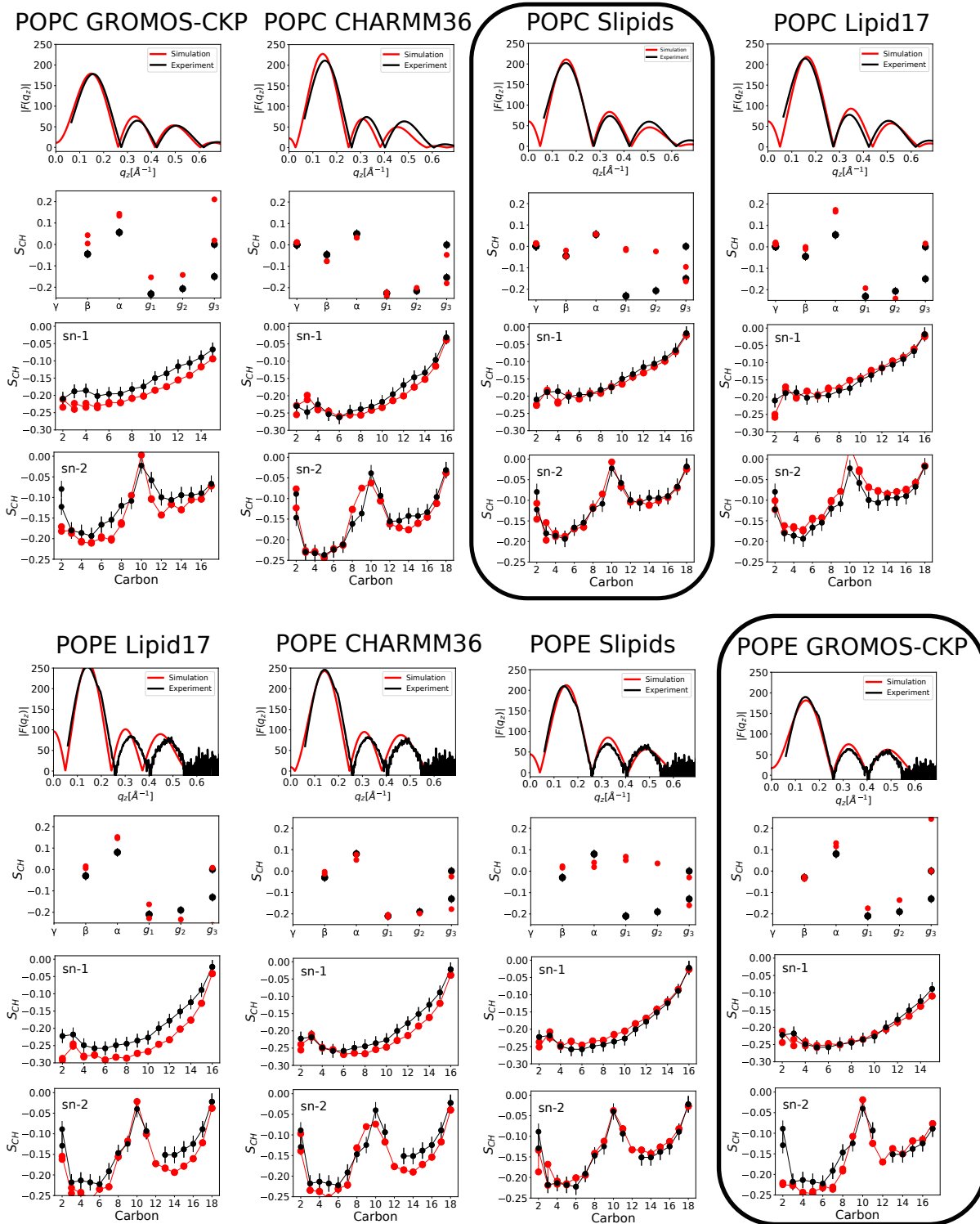


Figure S5. Simulations with the data for both POPC (top) and POPE (bottom) directly compared with the experimental data. The area per lipid increases from left to right. Simulations with the best overall quality for POPC and POPE order parameters are highlighted with a solid border.

S5 Testing machine learning models against literature data

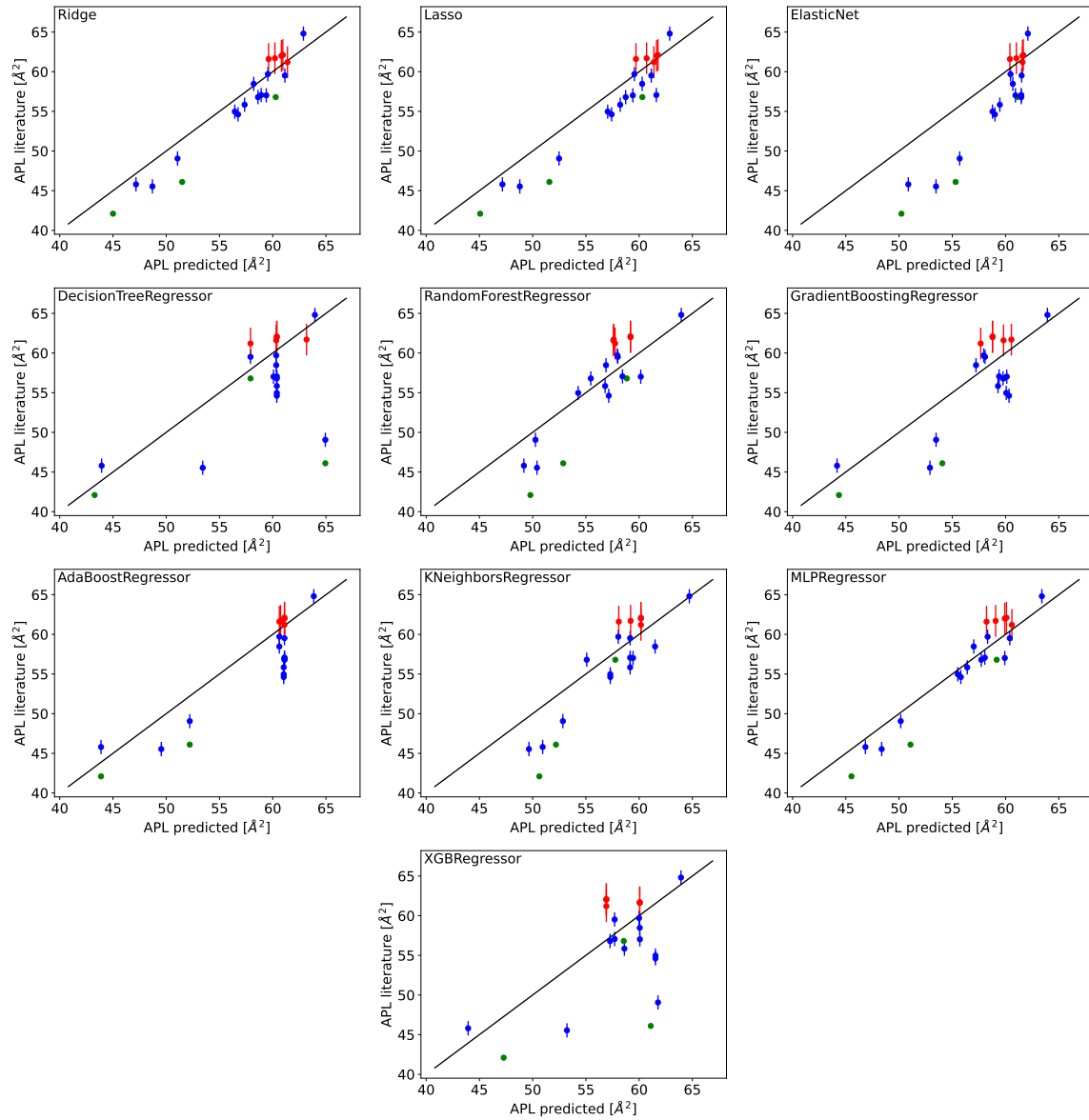


Figure S6. Predictions of area per lipids of POPC, POPE, POPS, PI, sphingomyelin lipids and cholesterol from the tested machine learning models against literature data from simulations (green², blue³, and red⁴).

S6 Water permeation through membranes

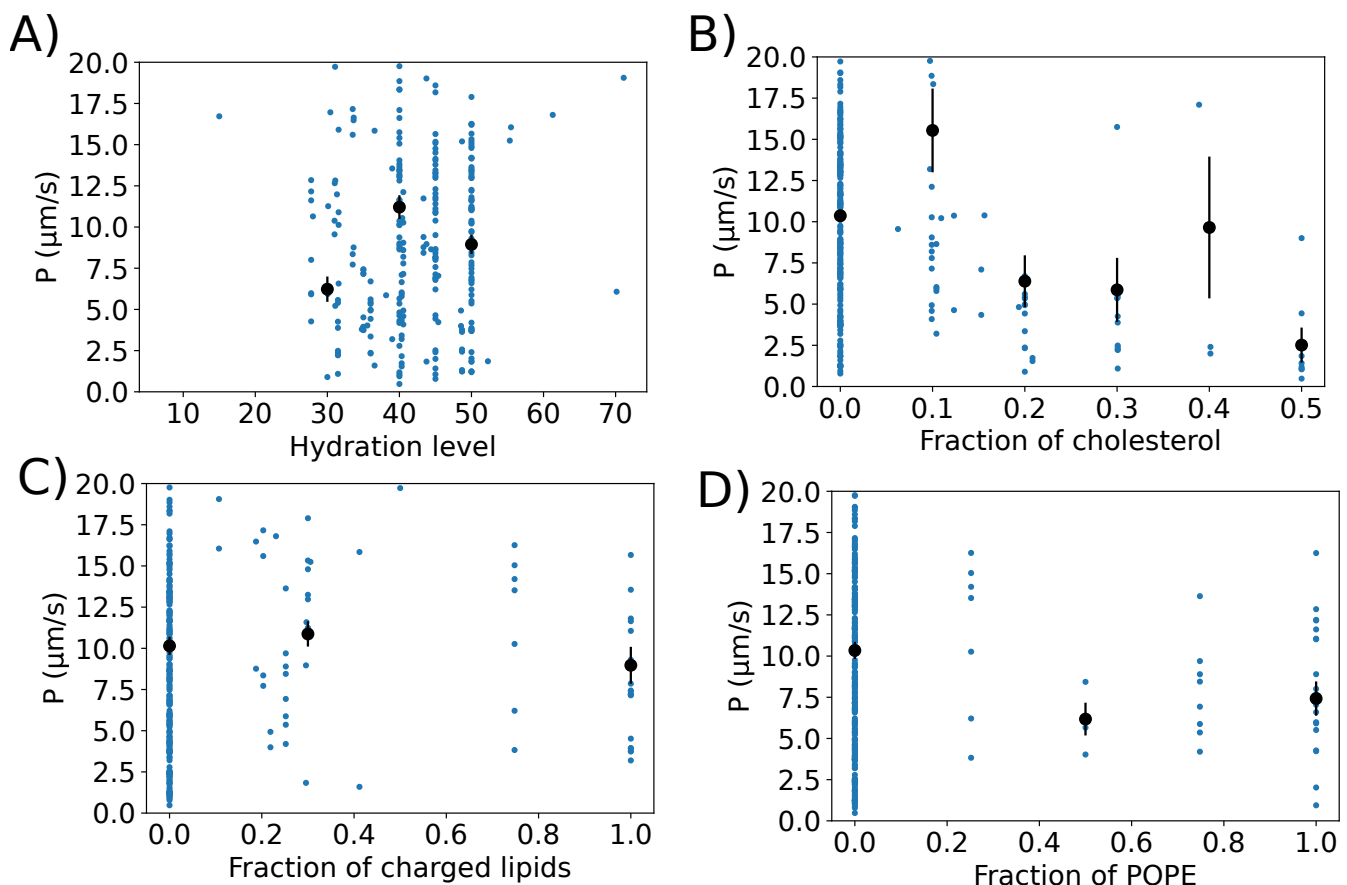


Figure S7. Water permeation through membranes analyzed from the Databank as a function of (A) hydration level, (B) fraction of cholesterol, (C) fraction of charged lipids, and (D) fraction of POPE in membrane. Values from simulations with non-zero permeation values are shown with blue dots. Histogrammed values are shown with black dots. For the mean value in each bin, average weighted with the simulation lengths was used, and error bars show the standard error of the mean. Only bins with more than one microsecond of data were used. Only simulations with the temperatures between 300-315 K were used.

S7 Water diffusion along membranes

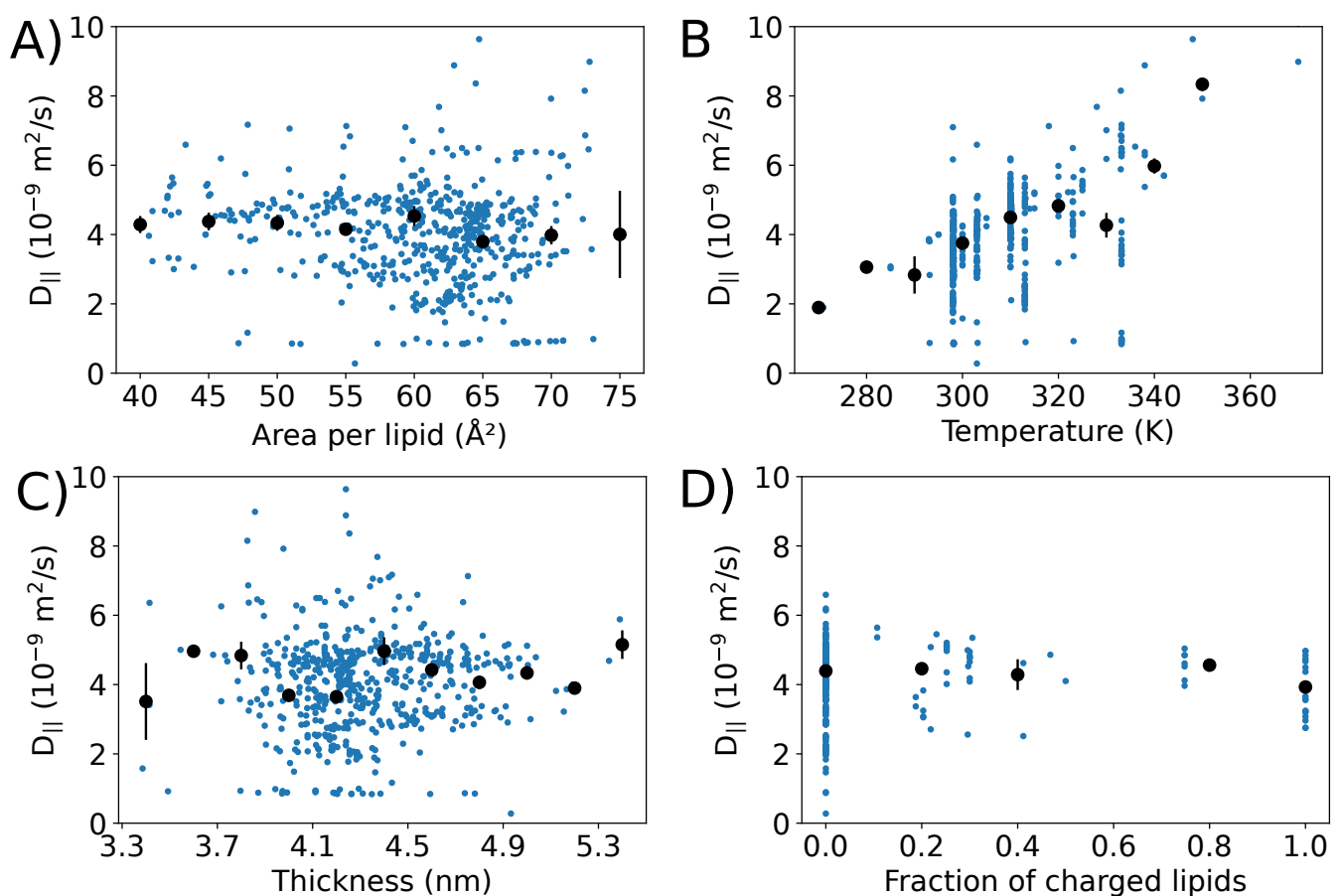


Figure S8. Lateral diffusion of water as a function of (A) area per lipid, (B) temperature, (C) membrane thickness, and (D) fraction of charged lipids in a membrane. Non-zero permeation and diffusion values from simulations are shown with blue dots. Histogrammed values are shown with black dots. For the mean value in each bin, average weighted with the simulation lengths was used, and error bars show the standard error of the mean. Only bins with more than one microsecond of data in total were used for water permeation. Only simulations with the temperatures between 300-315 K were used in D.

S8 Databank content

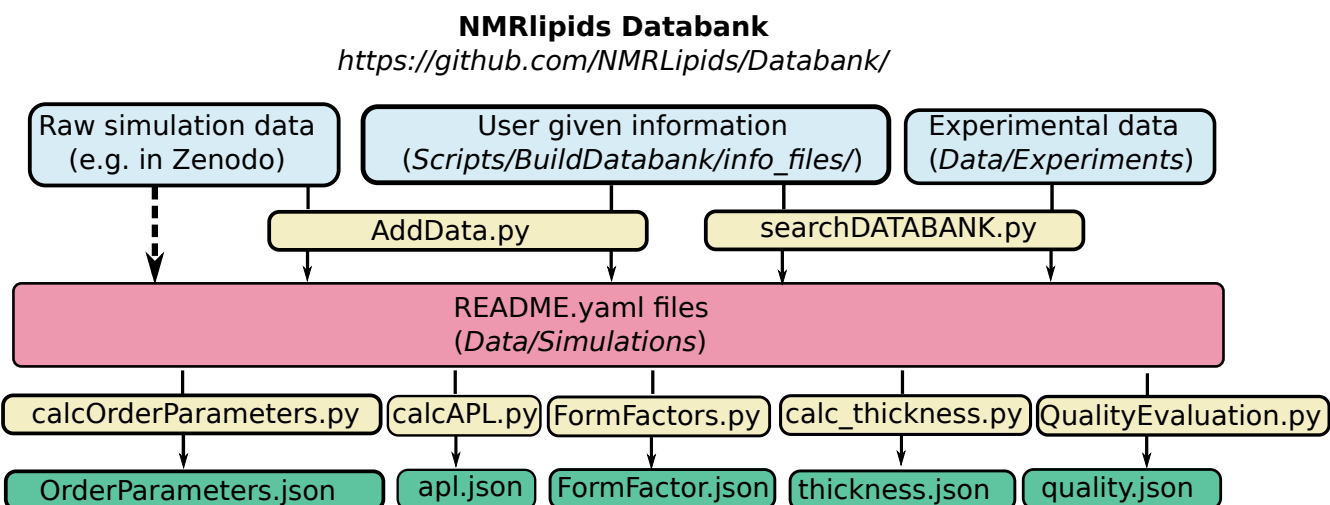


Figure S9. Structure of the NMRLipids Databank. Manually added input data (blue boxes) include basic information on the simulation, permanent links to the raw data, and experimental data if available. The databank entries (red box) and analysis results (green boxes), at <https://github.com/NMRLipids/Databank/tree/main/Data/Simulations> are automatically generated by the computer programs included in the NMRLipids Databank (yellow boxes). Because the raw data are not permanently stored but can be accessed based on the information in the Databank, this connection is marked with a dashed line.

| Code | Function | Input | Output |
|---------------------------------|--|-------------------|---|
| Databank layer | | | |
| Scripts/BuildDatabank/ | | | |
| AddData.py | Create README.yaml from user given information in info.yaml | info.yaml | README.yaml |
| searchDATABANK.py | Pair simulations with available experimental data | README.yaml files | Updated README.yaml files |
| QualityEvaluation.py | Quality-evaluate simulations that are paired with experimental data | README.yaml files | [lipid_name]_OrderParameters_quality.json, [lipid_name]_FragmentQuality.json, system_quality.json, FormFactorQuality.json |
| Scripts/AnalyzeDatabank/ | | | |
| calcOrderParameters.py | Calculate C-H bond order parameters for all lipids in the simulation | README.yaml files | [lipid_name]_OrderParameters.json |
| calcAPL.py | Calculate area per lipid as a function of time | README.yaml files | apl.json |
| calc_FormFactors.py | Calculate x-ray scattering form factors | README.yaml files | FormFactor.json |
| calc_thickness.py | Calculate membrane thickness | README.yaml files | thickness.json |

Table S1. List of relevant codes used to build the Databank and perform analyses in the *Databank layer* available at <https://github.com/NMRLipids/Databank/>.

| Code | Function | Input | Output |
|--|---|--|--|
| Application layer | | | |
| AreaPerLipidAndThicknessCorrelations.ipynb | Analyze correlations between results in the <i>Databank layer</i> | Results in the <i>Data-bank layer</i> | Figs. 2G and S2 |
| FlipFlop.py | Calculate flip-flop rates of lipids in all simulations | README.yaml | flipflop.dat files at /Data/Flipflops/ |
| plotFlipFlop.ipynb | Plot how flip-flop rates depend on membrane properties | README.yaml and flipflop.dat files at /Data/Flipflops/ | Fig. 4 |
| calcMD-PERMEATION.py | Calculate permeation rate of water molecules through bilayers from all simulations | README.yaml | Counting_events.txt files at /Data/MD-PERMEATION/ |
| calcWATERdiffusion.py | Calculate water lateral diffusion along membrane surface | README.yaml | WATERlateralMSD.xvg files at /Data/WATERdiffusion/ |
| plotWaterPermeation.ipynb | Plot how water permeation and diffusion depend on membrane properties | README.yaml, Count-ing_events.txt at /Data/MD-PERMEATION/ and WATERlateralMSD.xvg files at /Data/WATERdiffusion/ | Figs. 5, S7, and S8. |
| APLpredictor.ipynb | Predict area per lipid of a membrane based in its lipid composition from machine learning models trained using the NMRLipids databank | README.yaml and apl.dat files | Machine learning models at /Data/APLpredictor/ |

Table S2. Examples of codes that analyze membrane properties from the Databank in an *Application layer* available at <https://github.com/NMRLipids/DataBankManuscript/>.

| key | description | type |
|------------------|---|------------------------------|
| DOI | DOI from where the raw data is found | user given (compulsory) |
| SOFTWARE | Software used to run the simulation (Gromacs, Amber, NAMD, etc.) | |
| TRJ | Name of the trajectory file found from DOI (trr or xtc for Gromacs, dcd for OpenMM) | |
| TPR (Gromacs) | Name of the tpr topology file found from DOI for Gromacs simulations | |
| PDB (OpenMM) | Name of the pdb file found from DOI for OpenMM simulations | |
| PREEQTIME | Pre-equilibrate time simulated before the uploaded trajectory in nanoseconds. | |
| TIMELEFTOUT | Equilibration period in the uploaded trajectory that should be discarded in analyses. | |
| COMPOSITION | Dictionary connecting universal molecule and atom names to the ones used in simulation | |
| DIR_WRK | Temporary working directory in your local computer. | |
| UNITEDATOM_DICT | Information for constructing hydrogens for united atom simulations using buildH program ⁵ . Empty for all atom simulations. | |
| TYPEOFSYSTEM | Lipid bilayer or something else | |
| PUBLICATION | Give reference to a publication(s) related to the data | user given (optional) |
| AUTHORS_CONTACT | Name and email of the main author(s) of the data | |
| SYSTEM | System description on free text format | |
| SOFTWARE_VERSION | Version of the used software | |
| FF | Name of the used force field | |
| FF_SOURCE | Source of the force field parameters, e.g., CHARMM-GUI, webpage, citation to a publication | |
| FF_DATE | Date when force field parameters were accessed on the given source (day/month/year) | |
| FFmolename | Molecule specific force field information, e.g., water model with FFSOL and sodium parameters with FFSOD | |
| CPT | Name of the Gromacs checkpoint file | |
| LOG | Name of the Gromacs log file | |
| GRO | Name of the Gromacs gro file | |
| TOP | Name of top file for Gromacs or psf file for OpenMM | |
| CRD | Name of crd file for OpenMM | |
| WARNINGS | Dictionary containing information about unusual features in the trajectory, such as ambiguous atom names, membrane normal not oriented in z-direction, old Gromacs version used | |
| TRAJECTORY_SIZE | Size of the trajectory file in bytes | automatically extracted data |
| TRJLENGTH | Length of the trajectory (ps) | |
| TEMPERATURE | Temperature of the simulation | |
| NUMBER_OF_ATOMS | Number of atoms in the simulation | |
| DATEOFRUNNING | Date when added into the Databank | |
| EXPERIMENT | Potentially connected experimental data | |
| COMPOSITION | Numbers of lipid molecules in both leaflets and numbers of other molecules are added to the dictionary | |
| ID | Unique ID number to ease the analyses | |

Table S3. Keys stored in the README.yaml files of simulations.

| key | description |
|---------------------------|--|
| DOI | DOI of the publication related to the experimental data |
| TEMPERATURE | Temperature of the experiment |
| MOLAR_FRACTIONS | Dictionary of molar fractions of bilayer components |
| ION_CONCENTRATIONS | Dictionary of ion concentrations of the system |
| TOTAL_LIPID_CONCENTRATION | Total concentration of lipid components; if exact concentration is not known, but experiments are performed in excess water, 'full hydration' can be given |
| COUNTERIONS | Type of counter ions if present |

Table S4. Keys stored in the README.yaml files of experiments.

Force field name and references

CHARMM36⁶
 Slipids^{7–11}
 MacRog¹²
 Amber Lipid14/17^{13, 14}
 Charmm-Drude¹⁵
 ECCLipids^{16–18}
 GROMOS-CKP^{19–21}
 Berger²²
 ECC-CHARMM36²³
 Orange²⁴
 Poger²⁵
 GROMOS 43A1-S3²⁶
 GAFFlipid²⁷
 OPLS3e²⁸
 Ulmschneider²⁹
 Chiu Gromos²⁶
 AMOEBA³⁰
 OpenFF

Table S5. List of current force fields used in simulations in the Databank, with references.

S9 NMR experiments

Acyl chain order parameters of POPE (Figs. S10 and S11) and POPG (Figs. S12 and S13) were analyzed from the same data that were previously recorded to determine headgroup order parameters¹⁸. The analysis of the crowded spectral region at 29–31 ppm was based on the previous assignment reported for POPC membranes³¹. To measure the order parameters for DOPC (Fig. S14), the sample was prepared and experiments performed similarly to previous studies¹⁸.

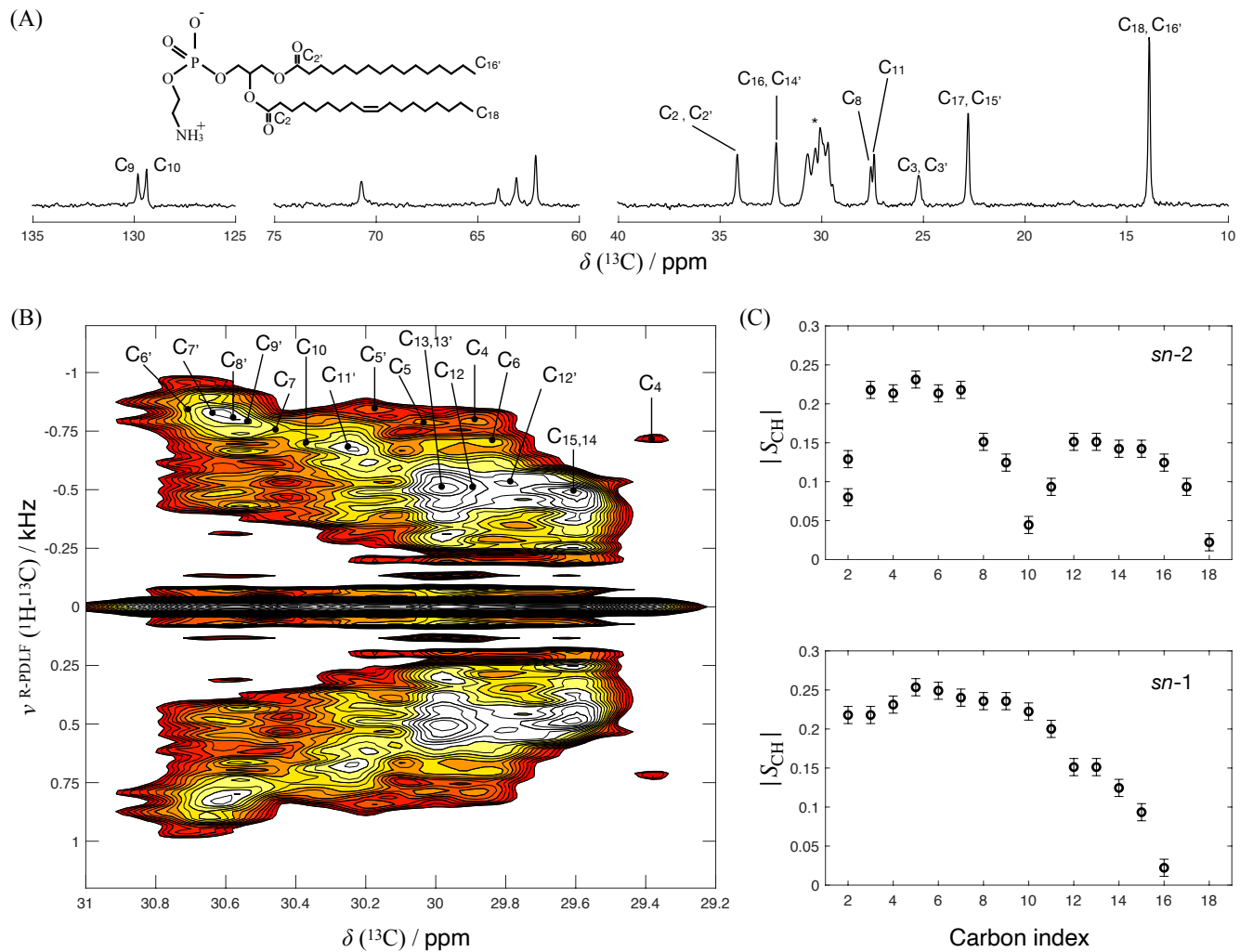


Figure S10. Determination of the POPE acyl chain order parameters from a R-PDLF spectrum measured at a magic angle spinning frequency of 5.15 kHz. (A) ^{13}C rINEPT spectrum with peak assignment. The labels used are shown in the chemical structure of POPE. The chemical shift of the methyl groups was defined as 13.8 ppm. (B) Contour plot of the R-PDLF spectrum for the crowded spectral region. The assignment was based on a previous assignment reported for POPC membranes³¹. (C) C–H bond order parameter profile for the acyl chains of POPE. The splittings used for calculating the order parameters are shown in Fig. S11. The unassigned peaks belong to the headgroup and glycerol backbone carbons. A detailed assignment and order parameter analysis of these carbons was shown previously¹⁸.

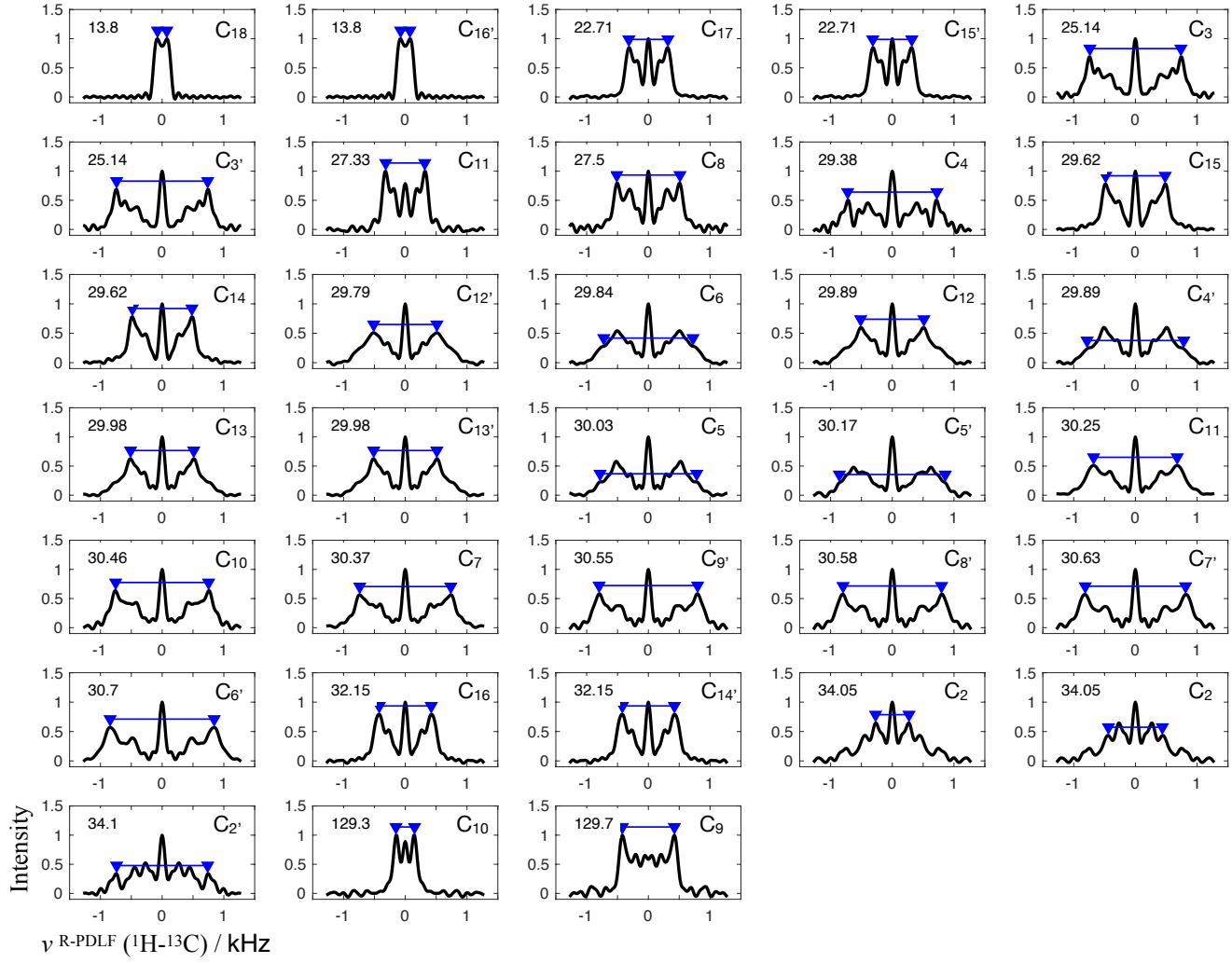


Figure S11. Dipolar spectra obtained from the 2D R-PDLF spectrum from POPE in Fig. S10. The number at the top left corner of each panel denotes the corresponding chemical shift. The carbon label for each splitting is displayed on the top right corner. The labels are the same as in Fig. S10.

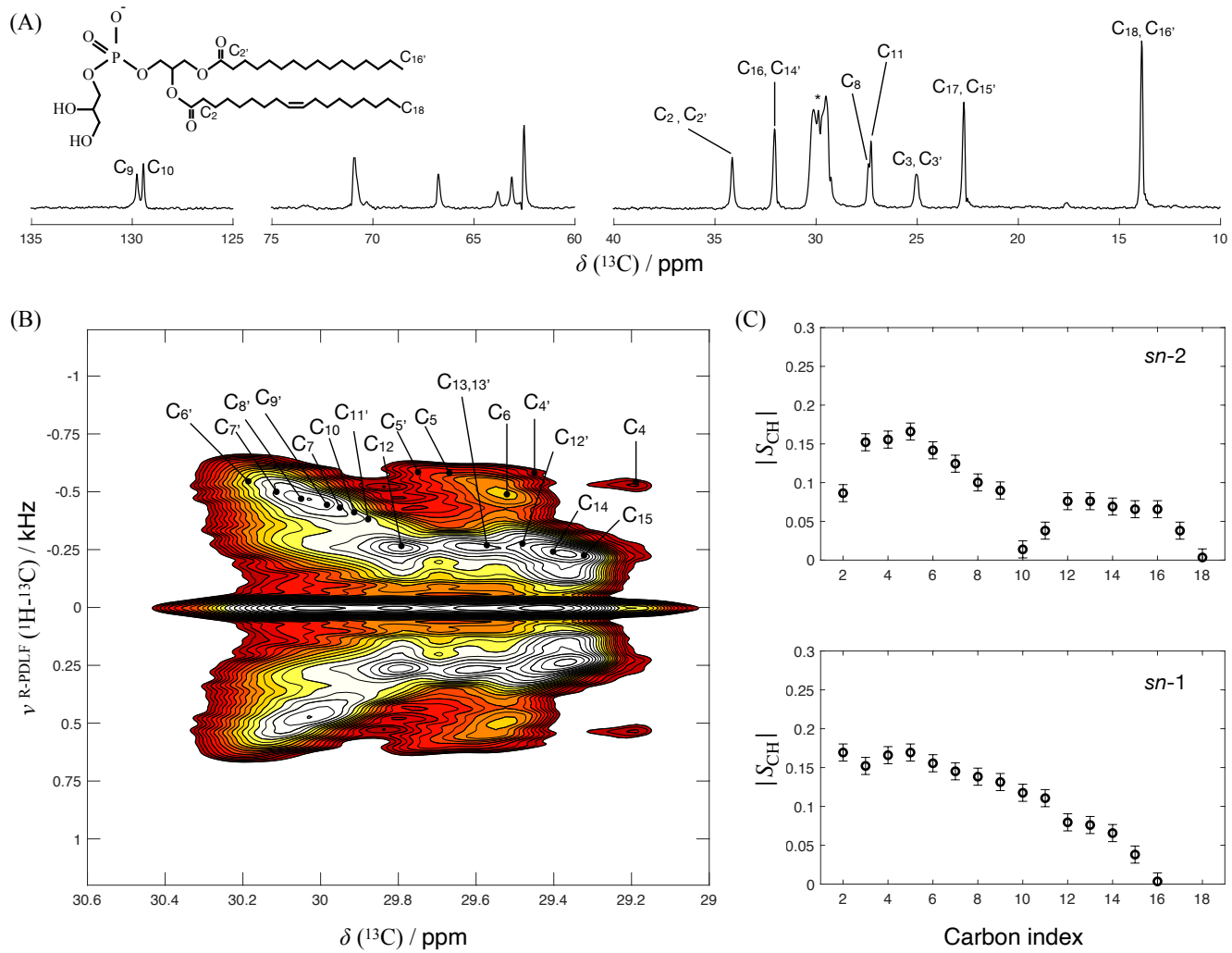


Figure S12. Determination of the POPG acyl chain order parameters from a R-PDLF spectrum measured at a magic angle spinning frequency of 5.15 kHz. (A) ^{13}C rIN EPT spectrum with peak assignment. The labels used are shown in the chemical structure of POPG. The chemical shift of the methyl groups was defined as 13.8 ppm. (B) Contour plot of the R-PDLF spectrum for the crowded spectral region. The assignment was based on a previous assignment reported for POPC membranes³¹. (C) C–H bond order parameter profile for the acyl chains of POPG. The splittings used for calculating the order parameters are shown in Fig. S13. The unassigned peaks belong to the headgroup and glycerol backbone carbons. A detailed assignment and order parameter analysis of these carbons was shown previously¹⁸.

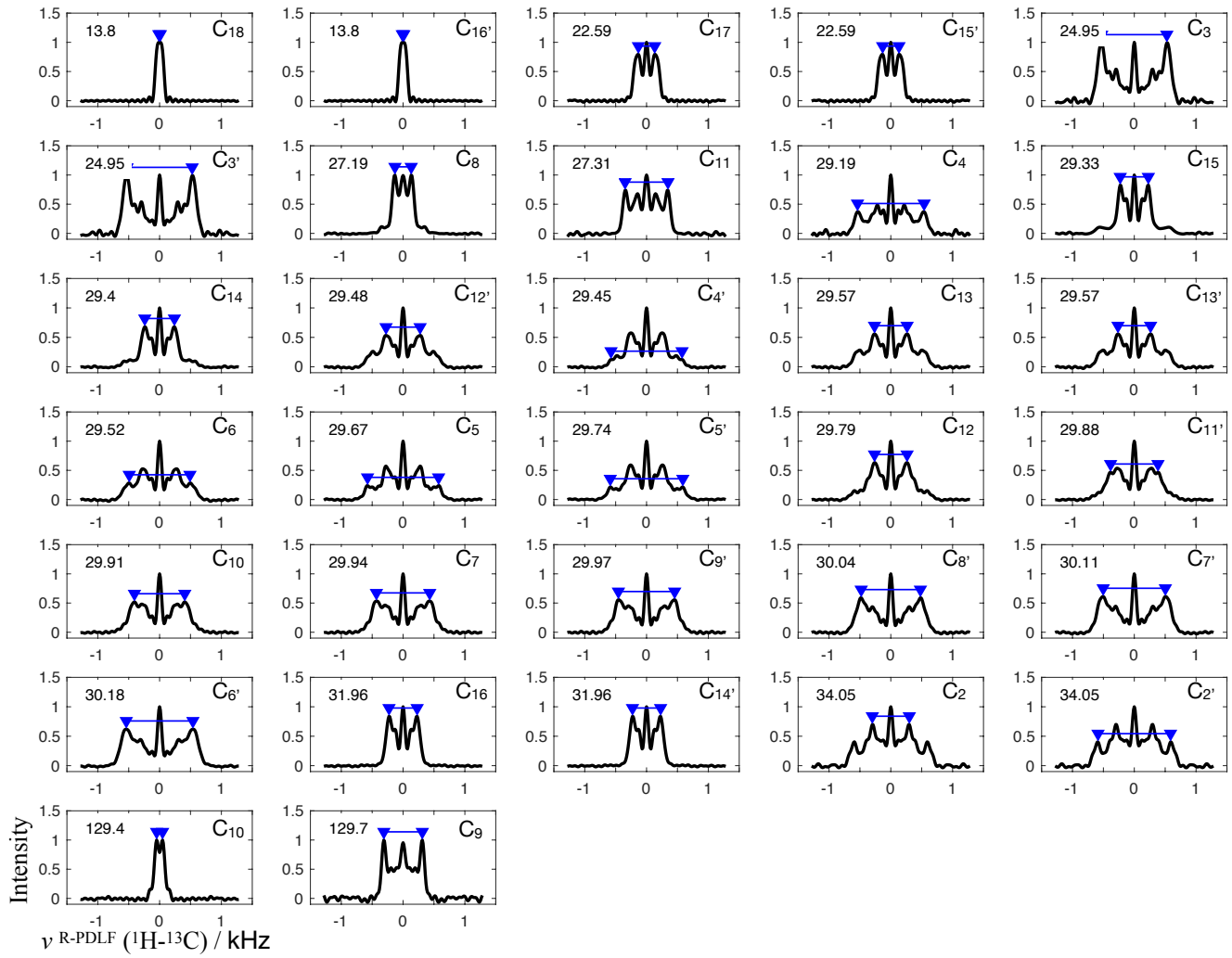


Figure S13. Dipolar spectra obtained from the 2D R-PDLF spectrum described in Fig. S12. The number at the top left corner of each panel denotes the corresponding chemical shift. The carbon label for each splitting is displayed on the top right corner. The labels are the same as in Fig. S12.

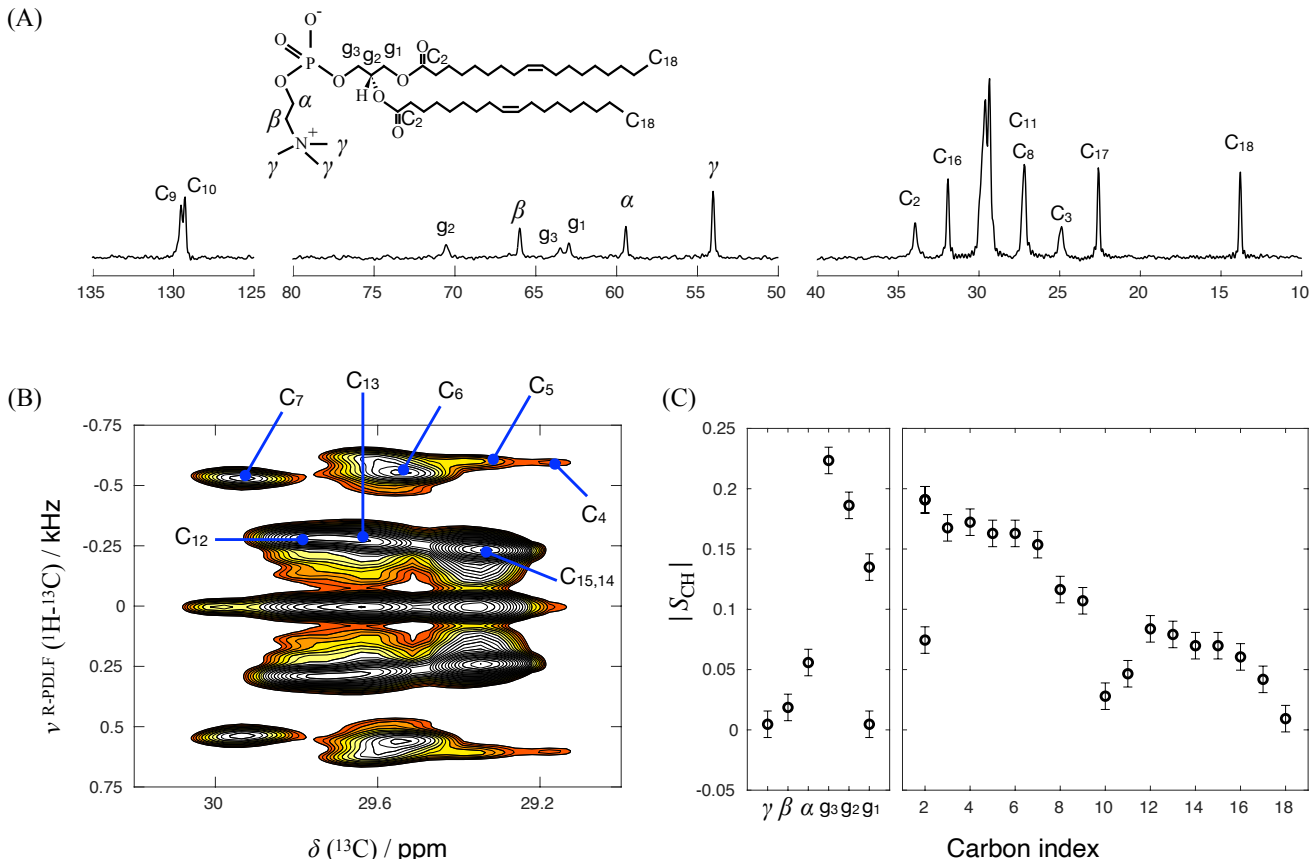


Figure S14. Determination of DOPC order parameters from a R-PDLF spectrum measured at a magic angle spinning frequency of 5.15 kHz. (A) ^{13}C rINEPT spectrum with peak assignment. The labels used are shown in the chemical structure of DOPC. The chemical shift of the methyl groups was defined as 13.8 ppm. (B) Contour plot of the R-PDLF spectrum for the crowded spectral region. The assignment was based on a previous assignment reported for POPC membranes³¹. (C) C–H bond order parameters of DOPC.

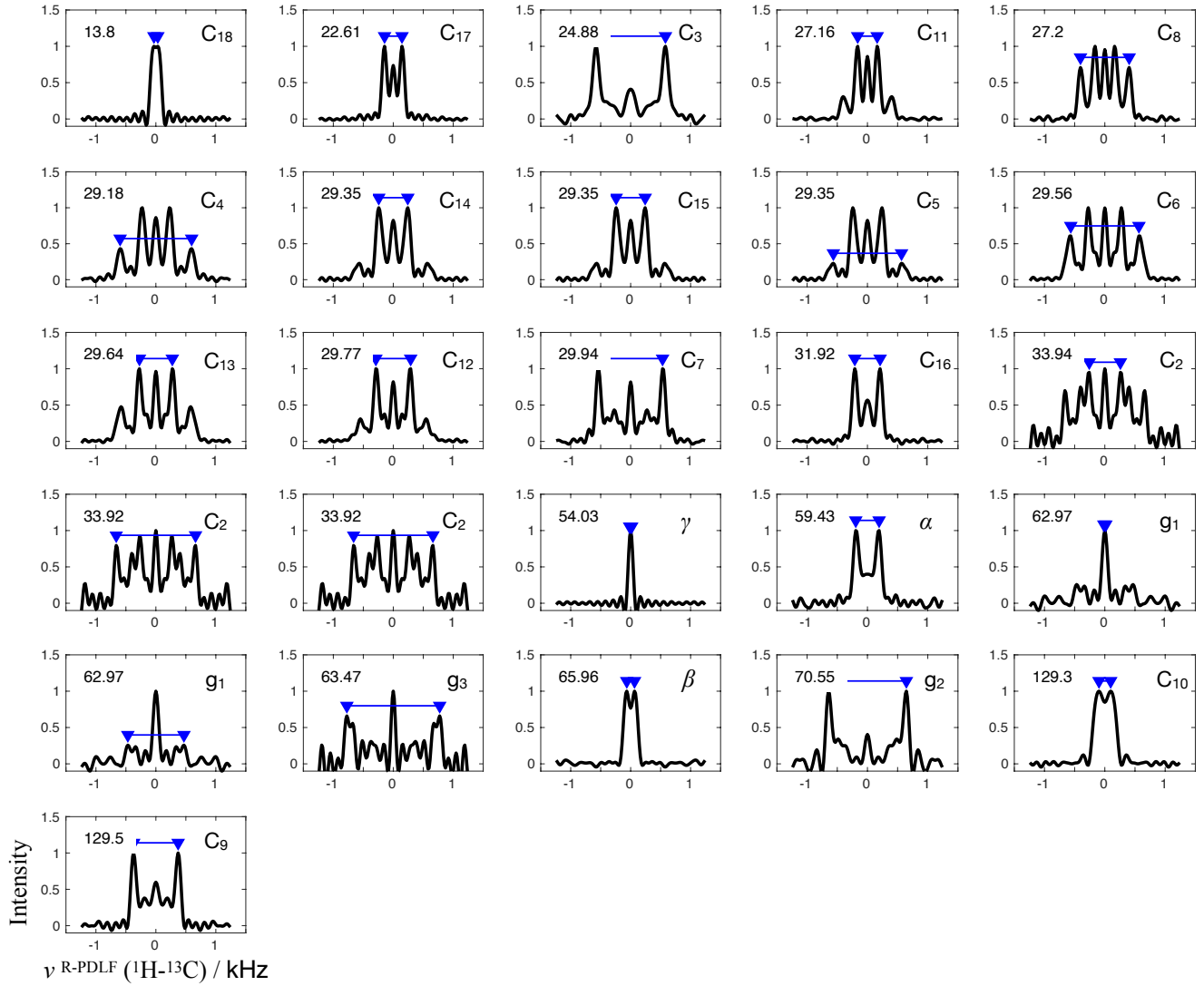


Figure S15. Dipolar spectra obtained from the 2D R-PDLF spectrum described in Fig. S14. The number at the top left corner of each panel denotes the corresponding chemical shift. The carbon label for each splitting is displayed on the top right corner. The labels are the same as in Fig. S14.

References

1. Javanainen, M. Simulations of POPC/cholesterol mixtures at 298 K, three system sizes, CHARMM36, DOI: [10.5281/zenodo.7035350](https://doi.org/10.5281/zenodo.7035350) (2021).
2. Shahane, G., Ding, W., Palaiokostas, M. & Orsi, M. Physical properties of model biological lipid bilayers: insights from all-atom molecular dynamics simulations. *J. Mol. Model.* **25**, 76 (2019).
3. Kumar, N. & Sastry, G. N. Study of lipid heterogeneity on bilayer membranes using molecular dynamics simulations. *J. Mol. Graph. Model.* **108**, 108000, DOI: <https://doi.org/10.1016/j.jmgm.2021.108000> (2021).
4. Oliveira, A. A. *et al.* Examining the effect of charged lipids on mitochondrial outer membrane dynamics using atomistic simulations. *Biomolecules* **12** (2022).
5. Santuz, H., Bacle, A., Poulain, P. & Fuchs, P. F. buildh: Build hydrogen atoms from united-atom molecular dynamics of lipids and calculate the order parameters. *J. Open Source Softw.* **6**, 3521, DOI: [10.21105/joss.03521](https://doi.org/10.21105/joss.03521) (2021).
6. Klauda, J. B. *et al.* Update of the CHARMM all-atom additive force field for lipids: Validation on six lipid types. *J. Phys. Chem. B* **114**, 7830–7843 (2010).
7. Jämbeck, J. P. M. & Lyubartsev, A. P. Derivation and systematic validation of a refined all-atom force field for phosphatidylcholine lipids. *J. Phys. Chem. B* **116**, 3164–3179 (2012).
8. Jämbeck, J. P. M. & Lyubartsev, A. P. An extension and further validation of an all-atomistic force field for biological membranes. *J. Chem. Theory Comput.* **8**, 2938–2948 (2012).
9. Jämbeck, J. P. & Lyubartsev, A. P. Another piece of the membrane puzzle: extending lipids further. *J. Chem. Theo. Comput.* **9**, 774–784 (2012).
10. Ermilova, I. & Lyubartsev, A. P. Extension of the lipids force field to polyunsaturated lipids. *The J. Phys. Chem. B* **120**, 12826–12842 (2016).
11. Grote, F. & Lyubartsev, A. P. Optimization of lipids force field parameters describing headgroups of phospholipids. *J. Phys. Chem. B* **124**, 8784–8793 (2020).
12. Kulig, W., Pasenkiewicz-Gierula, M. & Róg, T. Cis and trans unsaturated phosphatidylcholine bilayers: A molecular dynamics simulation study. *Chem. Phys. Lipids* **195**, 12 – 20 (2016).
13. Dickson, C. J. *et al.* Lipid14: The amber lipid force field. *J. Chem. Theory Comput.* **10**, 865–879 (2014).
14. Dickson, C. J., Walker, R. C. & Gould, I. R. Lipid21: Complex lipid membrane simulations with amber. *J. Chem. Theo. Comput.* **18**, 1726–1736 (2022).
15. Li, H. *et al.* Drude polarizable force field for molecular dynamics simulations of saturated and unsaturated zwitterionic lipids. *J. chemical theory computation* **13**, 4535–4552 (2017).
16. Melcr, J. *et al.* Accurate binding of sodium and calcium to a popc bilayer by effective inclusion of electronic polarization. *J. Phys. Chem. B* **122**, 4546–4557 (2018).
17. Melcr, J., Ferreira, T. M., Jungwirth, P. & Ollila, O. H. S. Improved cation binding to lipid bilayers with negatively charged pops by effective inclusion of electronic polarization. *J. Chem. Theo. Comput.* **16**, 738–748 (2020).
18. Bacle, A. *et al.* Inverse conformational selection in lipid–protein binding. *J. Am. Chem. Soc.* **143**, 13701–13709 (2021).
19. Chandrasekhar, I. *et al.* A consistent potential energy parameter set for lipids: dipalmitoylphosphatidylcholine as a benchmark of the gromos96 45a3 force field. *Eur. Biophys. J.* **32**, 67–77 (2003).
20. Kukol, A. Lipid models for united-atom molecular dynamics simulations of proteins. *J. Chem. Theory Comput.* **5**, 615–626 (2009).
21. Piggot, T. J., Piñeiro, Á. & Khalid, S. Molecular dynamics simulations of phosphatidylcholine membranes: A comparative force field study. *J. Chem. Theory Comput.* **8**, 4593–4609 (2012).
22. Berger, O., Edholm, O. & Jähnig, F. Molecular dynamics simulations of a fluid bilayer of dipalmitoylphosphatidylcholine at full hydration, constant pressure, and constant temperature. *Biophys. J.* **72**, 2002 – 2013 (1997).
23. Nencini, R. *Development and testing of computer models of phospholipid membranes*. Master's thesis, Charles University of Prague, DOI: <http://hdl.handle.net/20.500.11956/106127> (2019). [Http://hdl.handle.net/20.500.11956/106127](http://hdl.handle.net/20.500.11956/106127).
24. Catte, A. *et al.* Molecular electrometer and binding of cations to phospholipid bilayers. *Phys. Chem. Chem. Phys.* **18**, 32560–32569 (2016).

25. Poger, D., Van Gunsteren, W. F. & Mark, A. E. A new force field for simulating phosphatidylcholine bilayers. *J. Comput. Chem.* **31**, 1117–1125 (2010).
26. Chiu, S.-W., Pandit, S. A., Scott, H. L. & Jakobsson, E. An improved united atom force field for simulation of mixed lipid bilayers. *J. Phys. Chem. B* **113**, 2748–2763 (2009).
27. Dickson, C. J., Rosso, L., Betz, R. M., Walker, R. C. & Gould, I. R. GAFFlipid: a general amber force field for the accurate molecular dynamics simulation of phospholipid. *Soft Matter* **8**, 9617–9627 (2012).
28. Roos, K. *et al.* Opls3e: Extending force field coverage for drug-like small molecules. *J. Chem. Theory Comput.* **15**, 1863–1874 (2019).
29. Ulmschneider, J. P. & Ulmschneider, M. B. United atom lipid parameters for combination with the optimized potentials for liquid simulations all-atom force field. *J. Chem. Theory Comput.* **5**, 1803–1813 (2009).
30. Chu, H., Peng, X., Li, Y., Zhang, Y. & Li, G. A polarizable atomic multipole-based force field for molecular dynamics simulations of anionic lipids. *Molecules* **23**, 77 (2018).
31. Ferreira, T. M. *et al.* Cholesterol and POPC segmental order parameters in lipid membranes: solid state ^1H - ^{13}C NMR and MD simulation studies. *Phys. Chem. Chem. Phys.* **15**, 1976–1989 (2013).